Protein Cell 2010, 1(4): 393–405
DOI 10.1007/s13238-010-0038-6

Protein & Cell

RESEARCH ARTICLE

Interaction of the α2A domain of integrin with small collagen fragments

Hans-Christian Siebert[1] ✉, Monika Burg-Roderfeld[1], Thomas Eckert[1], Sabine Stötzel[1], Ulrike Kirch[1], Tammo Diercks[2,3], Martin J. Humphries[4], Martin Frank[5], Rainer Wechselberger[3], Emad Tajkhorshid[6], Steffen Oesser[7]

[1] Institut für Biochemie und Endokrinologie, Veterinärmedizinische Fakultät, Justus-Liebig-Universität Gießen, Frankfurter Str. 100, 35392 Gießen, Germany
[2] CiC bioGUNE, Parque Tecnológico de Bizkaia, Edificio 800, 48160 Derio, Spain
[3] Utrecht Facility for High-resolution NMR, Bijvoetcenter for Biomolecular Research Utrecht University, Padualaan 8, 3584CH Utrecht, The Netherlands
[4] Wellcome Trust Centre for Cell-Matrix Research, School of Biological Sciences, University of Manchester, 2.205 Stopford Building, Oxford Road, Manchester M13 9PT, UK
[5] Molecular Structure Analysis Core Facility, Deutsches Krebsforschungszentrum, Im Neuenheimer Feld 280, 69120 Heidelberg, Germany
[6] Department of Biochemistry, Beckman Institute, and Center for Biophysics and Computational Biology, University of Illinois at Urbana-Champaign, Urbana, IL, USA
[7] Collagen Research Institute, Schauenburgerstr. 116, D-24118 Kiel, Germany
✉ Correspondence: Hans-Christian.Siebert@vetmed.uni-giessen.de
Received February 18, 2010 Accepted March 27, 2010

ABSTRACT

We here present a detailed study of the ligand-receptor interactions between single and triple-helical strands of collagen and the α2A domain of integrin (α2A), providing valuable new insights into the mechanisms and dynamics of collagen-integrin binding at a sub-molecular level. The occurrence of single and triple-helical strands of the collagen fragments was scrutinized with atom force microscopy (AFM) techniques. Strong interactions of the triple-stranded fragments comparable to those of collagen can only be detected for the 42mer triple-helical collagen-like peptide under study (which contains 42 amino acid residues per strand) by solid phase assays as well as by surface plasmon resonance (SPR) measurements. However, changes in NMR signals during titration and characteristic saturation transfer difference (STD) NMR signals are also detectable when α2A is added to a solution of the 21mer single-stranded collagen fragment. Molecular dynamics (MD) simulations employing different sets of force field parameters were applied to study the interaction between triple-helical or single-stranded collagen fragments with α2A. It is remarkable that even single-stranded collagen fragments can form various complexes with α2A showing significant differences in the complex stability with identical ligands. The results of MD simulations are in agreement with the signal alterations in our NMR experiments, which are indicative of the formation of weak complexes between single-stranded collagen and α2A in solution. These results provide useful information concerning possible interactions of α2A with small collagen fragments that are of relevance to the design of novel therapeutic A-domain inhibitors.

KEYWORDS integrin-collagen interaction, NMR, SPR, AFM, molecular modeling

INTRODUCTION

The α2A domain of integrin (α2A) exhibits specific binding to triple-helical collagen fragments. Similar to the complete receptor (full integrin), binding by α2A is cation-dependent, mainly supported by cobalt, magnesium, or manganese, but less by calcium (Calderwood et al., 1995; Dickeson et al., 1997). A specific collagen motif recognized by α2A has been identified as the GFOGER (O: hydroxyproline) motif within the context of a triple helix (Emsley et al., 2000). On the basis of these findings we investigated ligand interaction with α2A using larger (42mer) and smaller (21mer) collagen fragments. Collagen receptors such as α2A, discoidin 1 and 2 (Vogel

et al., 2006; Ichikawa et al., 2007; Kiedzierska et al., 2007; Leitinger and Hohenester, 2007) as well as the von-Willebrand factor (Huizinga et al., 1997; Romijn et al., 2001; Nishida et al., 2003), bind in a specific way to triple-helical collagen strands like the 42mer collagen fragment. In contrast, integrin V (Xiong et al., 2002) appears to be a collagen receptor with specificity for degraded collagen, as it binds to single-stranded, collagen-like peptides. Integrins have in common that they recognize a defined part on the collagen structure, as demonstrated for, e.g., α5β1 and α1β1 integrin (Humphries et al., 2000; Coe et al., 2001; Kim et al., 2005). Regarding the architecture of the binding pocket of α2A, it is not completely clear why single-stranded collagen fragments are unable to establish a stable specific binding interaction with this receptor. Since collagen fragments are present in various compartments in living organisms, and given their therapeutic relevance, the answer to this question is of special interest. The preferred binding of triple-helical strands to α2A might be due to one or a combination of several molecular reasons: (1) the rigidity of the triple-helical structure compared to single-stranded collagen; (2) the stabilization of a binding conformation in a triple-helical structure; and (3) the occurrence of optimal positions for crucial interacting amino acids in both ligand and receptor. Furthermore, it is currently unclear whether a weak, but specific binding of α2A to single-stranded collagen strands is principally excluded. We show that such weak binding can be detected by NMR-methods and described in detail by MD simulations.

RESULTS

The 42mer collagen fragment binds to α2A in a specific manner, as clearly detected by surface plasmon resonance (SPR) experiments (Fig. 1A and 1B as well as Supplemental Fig. 1A–C and Supplemental Fig. 2). The interaction of α2A with immobilized collagen fragments was measured using the XPR36 ProteOn system. The protein α2A was simultaneously injected at several concentrations at the same time in different channels over immobilized 42mer collagen fragments in the presence of divalent ions using a one-shot kinetic analysis provided by the XPR36 system. Six channels were available

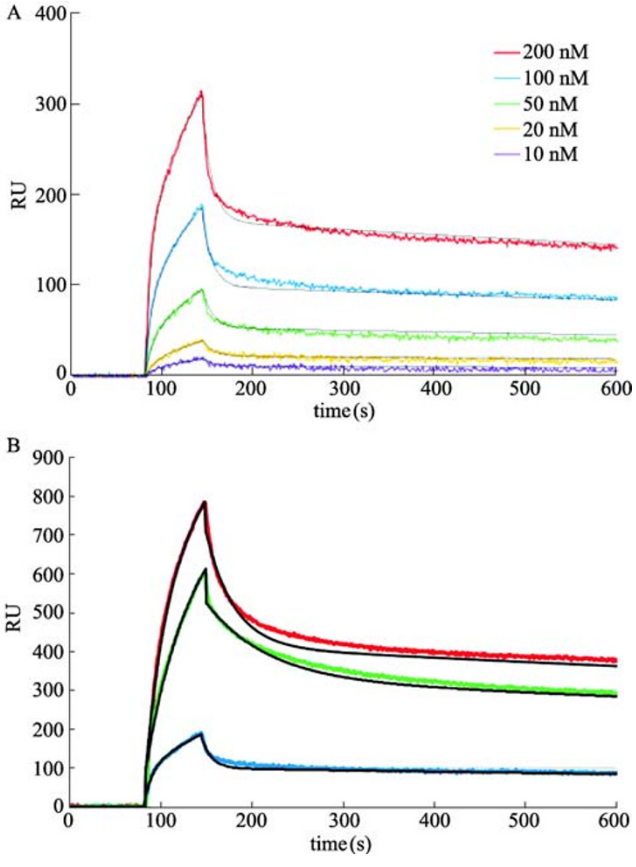

Figure 1. Kinetic results on the interaction between the 42mer collagen fragment and α2A. (A) Binding curves of 200 nM (red), 100 nM (blue), 50 nM (green), 20 nM (yellow) and 10 nM (purple) α2A interacting with ~1900 RU immobilized 42mer collagen fragment in the presence of 2 mM Mg^{2+} ions. (B) Interaction of 100 nM α2A with ~1900 RU immobilized 42mer collagen fragment in the presence of 2 mM Co^{2+} (red), 2 mM Mn^{2+} (green) and 2 mM Mg^{2+} ions (blue), respectively. The corresponding fitted curves are presented as black solid lines.

in vertical and horizontal directions, respectively (Nahshol et al., 2008). The collagen fragment was immobilized on one channel in the horizontal direction, while capturing of α2A occurred in the vertical orientation. One separate channel was taken for each concentration, thus, enabling parallel data collection. Additionally, one channel was prepared for data referencing, thereby activating this channel followed by an immobilization step without protein and a final deactivation with ethanolamine. Our data clearly show that the 42mer collagen fragments interact in a concentration-dependent manner. Kinetic analysis using the two-state model revealed that the fitted curves obtained from the calculation were congruent with the raw data sets.

Variations of the ion type show dramatic effects on the binding capacities of α2A to the 42mer collagen fragment (Fig. 1B). The apparent values of the kinetic analysis resulting from one-shot kinetic experiments with Co^{2+}, Mn^{2+} and Mg^{2+} are displayed in Table 1 (data for Ca^{2+} ions are not shown). No binding was detected in the absence of any divalent cations.

The so-called open state conformation of α2A represents the high affinity GFOGER-binding form, while the closed state represents the inactive form that barely binds GFOGER. The association rates calculated from our SPR data show that Co^{2+} ions result in a higher k_{on} value than the other ions, pointing to a faster association. In the presence of Co^{2+} ions, a relatively high k_{off} value was also calculated, which is characteristic of fast dissociation of the complex. In contrast, we measured a smaller dissociation rate in the presence of Mn^{2+} ions, reflecting the presence of a more stable complex under these conditions. However, we have also detected a

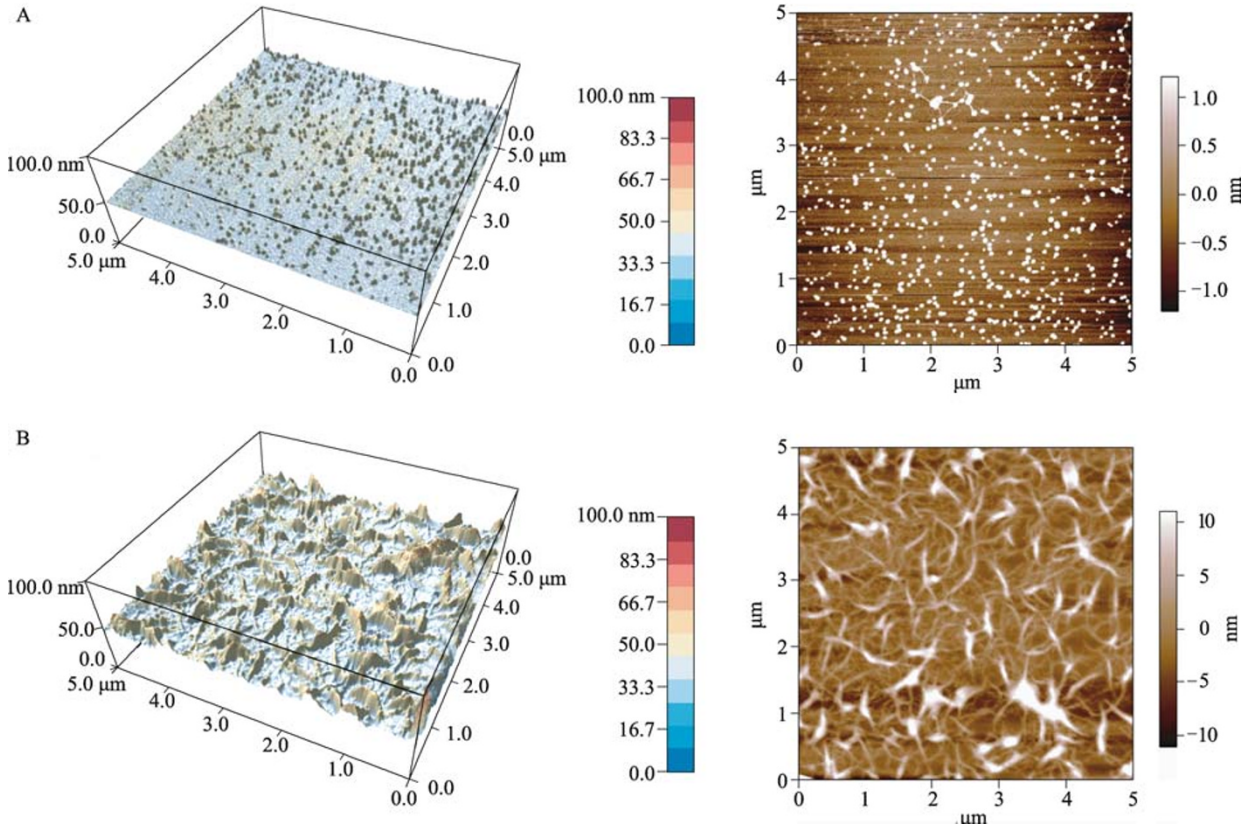

Figure 2. AFM images of 21mer and the 42mer collagen fragments. (A) AFM images of small collagen fragments with 21 residues that do not show any triple-helical structure. (B) AFM images of the 42mer collagen fragments that forms fibrillar structures. The left panel shows a three-dimensional view and the right one a two-dimensional presentation.

Table 1 Kinetic parameters describing the interactions between the 42mer collagen fragment and the α2A domain

	open state conformation			close state conformation		
cations (2 mM)	k_{on} (10^4 $M^{-1}s^{-1}$)	k_{off} (10^{-3} s^{-1})	KD (nM)	k_{on} (10^{-2} $M^{-1}s^{-1}$)	k_{off} (10^{-4} s^{-1})	KD (mM)
Mg^{2+}	15.2 ± 0.27	90.0 ± 1.8	575	2.0 ± 0.01	4.8 ± 0.06	30
Mn^{2+}	3.1 ± 0.02	8.5 ± 0.2	276	0.8 ± 0.01	7.2 ± 0.15	90
Co^{2+}	20.3 ± 0.15	20.0 ± 0.4	121	1.0 ± 0.01	4.8 ± 0.07	40

small association rate indicating that the complex formation is slower than in the presence of the two other ions. Compared to Mn^{2+} and Co^{2+}, a weaker complex was formed in the presence of Mg^{2+}, as shown by the highest dissociation rate in Table 1. However, in all cases the affinity of the closed form was about 10^5 times weaker than the open conformation.

When SPR experiments and solid phase assays were carried out for collagen fragments like the 21mer peptide (GPOGPOGFOGERGPOGPOGPO), no specific binding with α2A was detectable. Only for fragments longer than 30 residues per strand (e.g., the 42mer collagen fragment) with a clear triple-helical structure, it was possible to detect specific interactions by SPR experiments and in solid phase assays. This result is in complete agreement with the literature (Berisio et al., 2002; Persikov et al., 2005). As additional control experiments, we performed SPR measurements in which the α2A domain was immobilized. The 42mer collagen fragments were found to be stably bound by α2A (Supplemental Fig. 1). In order to directly visualize the differences between the aggregation behaviours and in the molecular organizations of the 21mer and the 42mer collagen fragments, we performed AFM experiments (Fig. 2).

Tapping mode AFM measurements of thin collagen fragment films on mica demonstrated a marked difference between the small (21mer) and the large (42mer) collagen fragments (Fig. 2A and 2B, respectively). Comparison of two- and three-dimensional AFM images of 5 μm × 5 μm areas of collagen fragments on mica indicated the presence of fibrillar structures only in the case of the large collagen fragments (Fig. 2B). In contrast, no fibrillar structures were obtained from small collagen fragments (Fig. 2A).

One-dimensional proton NMR spectra of a 21mer collagen fragment in its triple-helical or single-stranded form in the absence and in the presence of α2A were compared with each other. Distinct signal alterations (significant differences in the chemical shift values) were detected especially for the Arg-signals (Fig. 3). These observations indicate molecular interactions between ligand and receptor.

Increasing of the half width line broadenings of certain NMR signals as well as signal shift alterations were analyzed

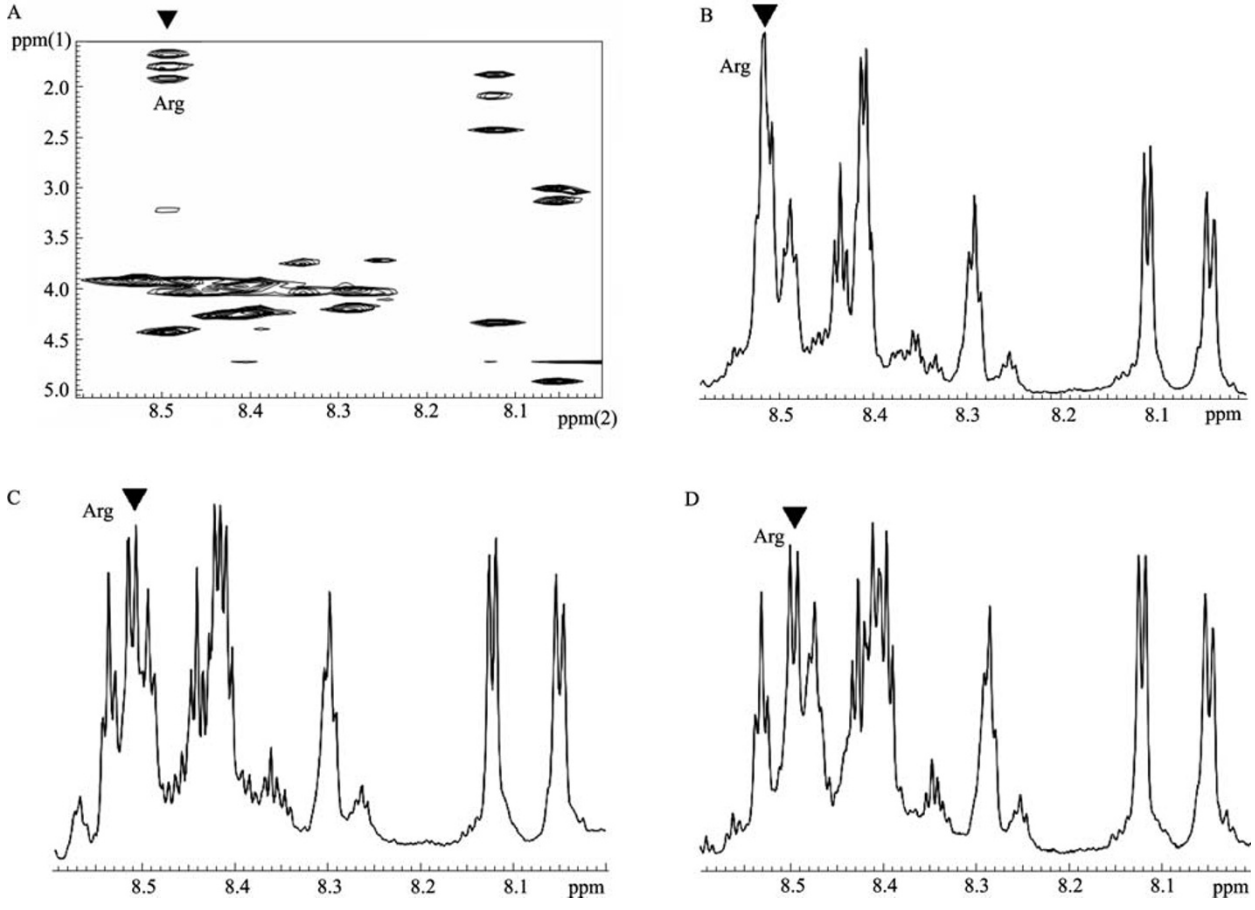

Figure 3. NMR spectra of the 21mer collagen fragment in the presence of the α2A domain of integrin. NMR spectra of the 21mer collagen fragment were recorded in the absence (A, B) and in the presence (C, D) of the α2A domain of integrin. The crucial part of the receptor-free collagen fragment 2D proton NMR spectrum (A) corresponds that of the receptor-free 1D spectrum (B). The molar ratio between ligand and receptor is one-molar (C) and two molar (D) excess of α2A.

qualitatively. Results of a quantitative analysis as revealed by a detailed NMR-titration study will be presented in a follow-up study in which also other integrin domains are analyzed. The measured signal alterations argue in favor of a specific binding effect since only certain signals (e.g., those of the Arg-residue) are involved.

Saturation transfer difference (STD) NMR experiments with various collagen fragments from a collagen-hydrolysate confirmed that arginine residues from the ligand structures are gripped in molecular interactions with α2A in solution (Fig. 4).

Molecular interactions underlying the observed weak binding between the 21mer collagen fragment and α2A in NMR experiments were simulated with molecular dynamics (MD) calculations. First we analyzed the build-up of triple-helical collagen fragments at sizes between 20 and 30 amino acid residues, thereby testing the potential of single collagen strands to form hydrogen bonds. The corresponding model structures were designed in accordance with the parameters of the complex-structures described in the methods part. The collagen chains were constructed from proline, hydroxyproline and glycine only. A snapshot of these MD simulations is shown in Fig. 5.

The units remain stable in their trimeric twisted form. Stabilization is caused by Hyp-Pro stacking and Gly-Pro/Hyp H-bonds. The trimeric units form clusters with each other. The specific interactions between the different strands are mediated by H-bonds mainly involving the hydroxyl groups of the hydroxyproline (Hyp) residues. Inter-trimeric stacking interactions of Pro/Hyp residues also stabilize the cluster, leading to a relative rigidity of these fragments. At chain length of 30 residues, the modeled triple-helical strands seem to organize and aggregate in a similar way to what was deduced from our AFM observations.

As a suitable starting structure for the MD simulations of a collagen fragment receptor complex we have chosen the X-ray derived structural model of the 21mer peptide interacting in its triple-helical form with α2A (PDB code: 1DZI). Examining the interaction of collagen fragments with the collagen binding pocket of α2A (Fig. 6) during the simulations, we observed that up to five amino acids in a single strand can interact simultaneously with crucial residues in the binding pocket of α2A.

From the model, it is not clear why a small single-stranded collagen fragment should not be suited to maintain a specific

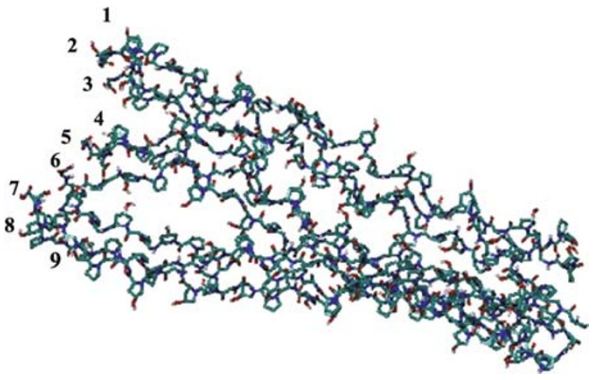

Figure 5. Snapshot from a GROMACS MD simulation of nine collagen fragments in water. Water molecules are not shown.

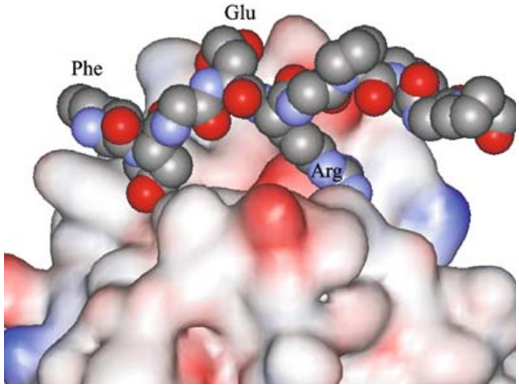

Figure 6. Single stranded collagen fragment in the binding pocket of α2A. Chain B in 1DZI is drawn in a van-der-Waals representation colored by atom types: carbon (grey), oxygen (red), nitrogen (blue).

interaction with the binding pocket of α2A in its collagen binding conformation (Fig. 6).

MD simulations were performed initially on the complex of trimeric collagen and α2A. A snapshot taken from the end of this simulation is shown in Fig. 7 and Supplemental Fig. 3.

During the simulations of triple-stranded collagen fragments with α2A, the complex was found to be stable and exhibited similar dynamics in simulations employing different force fields (CHARMM or GROMOS 96 ffG43a1). We

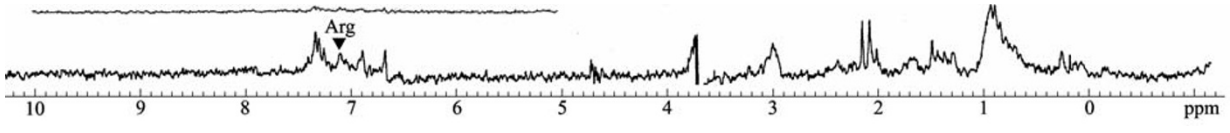

Figure 4. STD spectrum of collagen fragments from a collagen-hydrolysate in the presence of the α2A domain of integrin. The molar ratio between ligand and receptor is 50:1. The crucial part of the corresponding off-resonance spectrum is inserted above the STD spectrum for comparison.

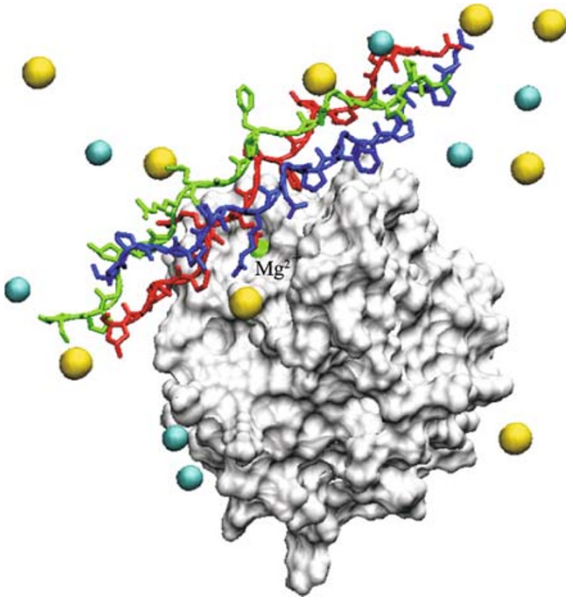

Figure 7. Snapshot taken from the simulation of the complex of trimeric collagen and α2A (1DZI.pdb as the starting structure) performed with NAMD. The placed Mg^{2+} is shown as a green sphere, and α2A (A-chain in the PDB file) is shown in a surface presentation. In collagen, chains B, C and D are drawn in blue, red, and green, respectively. Na^{+} (cyan) and Cl^{-} (yellow) ions are drawn as spheres. Water molecules are not shown (for comparison see also Supplemental Fig. 3).

continued our MD analysis with simulations in which only one of the three collagen strands in 1DZI.pdb was kept while the other two were deleted. The three collagen strands are sequence-wise identical, but arranged in different positions in respect to the collagen binding pocket of α2A. A number of MD simulations were performed to examine the dynamics of individual collagen chains. Our structural comparison of the C-chain in complex with integrin is displayed as snapshots taken from MD runs of two different programs (Fig. 8).

The C-chain-α2A complex is stable due to a strong interaction between a specific glutamate of the collagen fragment and the Mg^{2+} cation in α2A throughout the simulation (Fig. 8 and Supplemental Fig. 4). However, this contact seams not to play a key role in the weak binding interactions according to our NMR results (Fig. 3), since the chemical shift alterations are independent of the cation concentration. Therefore, we focused on MD simulations of the monomeric B- and D-chain where the interactions with α2A are not supported by any cations. Moreover, the starting structures of the complexes with the single strands B or D were arranged in a position and conformation given by the X-ray data file 1DZI.pdb. A complex between chain B and α2A is unstable during the MD simulation although the arginine from the collagen strand is in a proper binding position. Here, the number of hydrogen bonds, which are also responsible for the formation of a triple-helical structure, is insufficient between the B-chain and α2A (Fig. 5). The complex between B chain and integrin domain loses its stability in the second half of the simulation, and the collagen fragment disentangles from its receptor (Fig. 9).

The interactions between single-stranded collagen fragments and the integrin domain under study can be analyzed in detail by examining the simulated trajectory of the D-chain interacting with α2A (Fig. 10). During the simulation, an

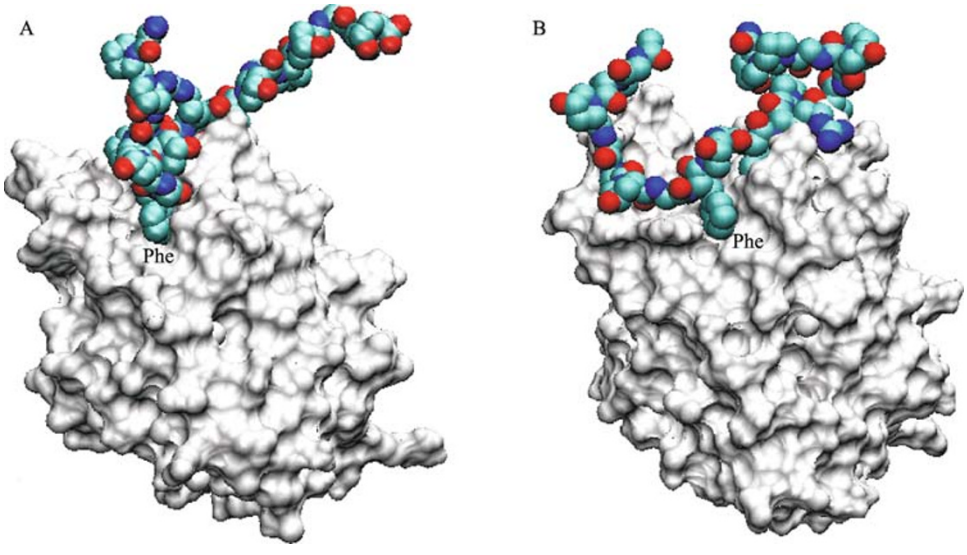

Figure 8. Single stranded collagen fragment (C-chain) in the binding pocket of α2A (1DZI.pdb). Snapshots are taken from two independent simulations, one performed with GROMACS (A) and the other with CHARMM (B). For a better orientation we have labelled the Phe-residue of the C-chain.

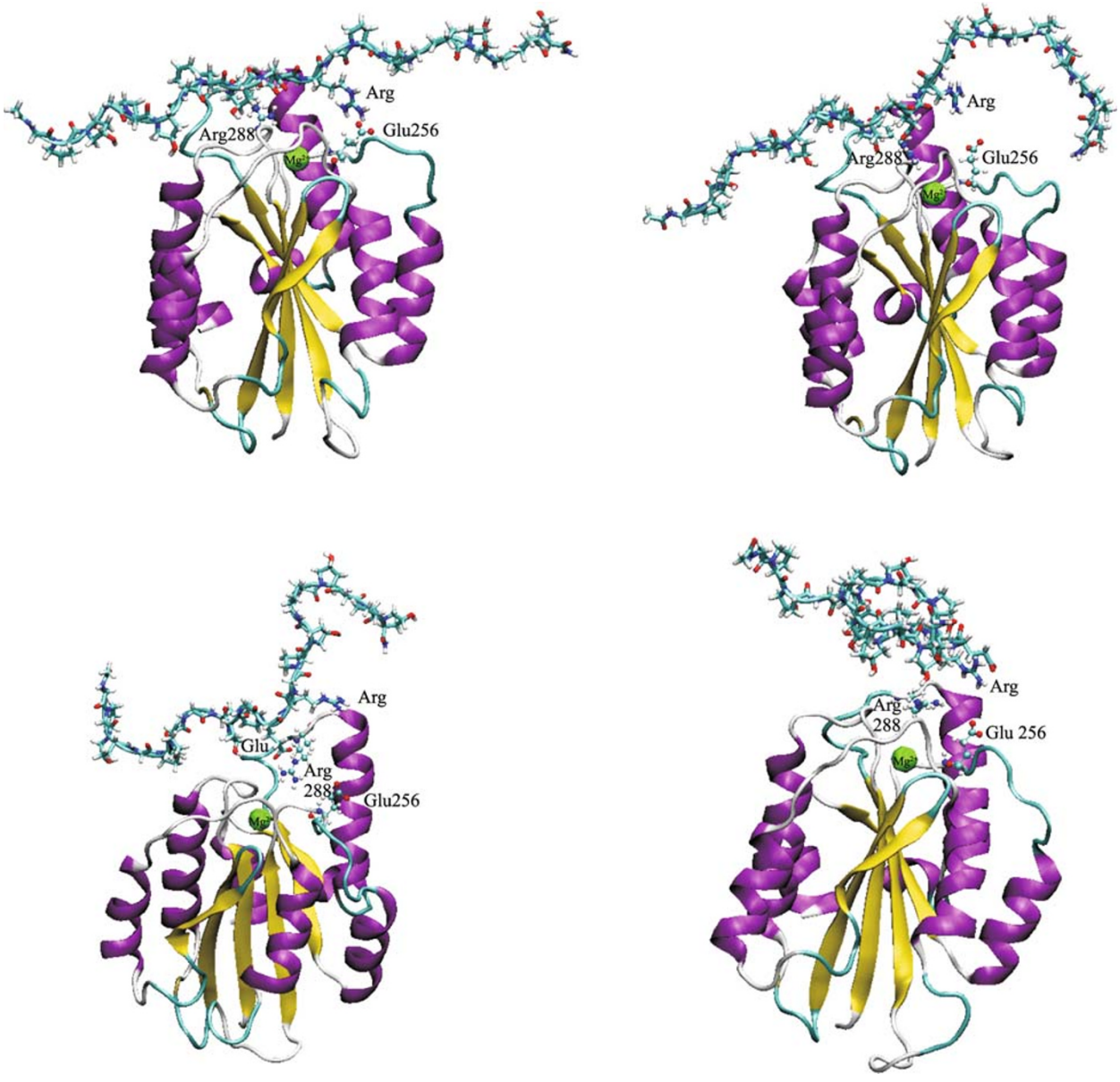

Figure 9. Single stranded collagen fragment (B-chain) in the binding pocket of the integrin α2A domain (1DZI.pdb). Snapshots are taken at four different states of the NAMD simulation. The sequence of the 21mer single strand is GPOGPOGFOGERGPOGPOGPO.

arginine at position 12, which is initially not in contact with the α2A integrin domain, established a salt-bridge with Glu256 of α2A. After this stable contact has been formed it survives until the end of the simulation (Fig. 10) pointing to an important role for Arg12 of the collagen fragment in binding to α2A.

Differences in the binding behavior between the B-, C- and D-chain in respect to the α2A domain of integrin could be a result of crystallographic effects. However, it is of notice that diverse ligand-receptor positions on the basis of the X-ray crystallographic data (1DZI.pdb) lead to the alterations in the binding process as documented by our MD simulations.

Movies of all our NAMD simulations on the described complexes can be downloaded under: www.life.uiuc.edu/emad/integrin-collagen.

DISCUSSION

In this study we report the first detailed kinetics analysis of α2A interactions with triple-helical and monomeric collagen fragments containing the GFOGER-motif in the presence of different divalent ions. This motif is postulated to select and stabilize the open state conformation of α2A within a ligand-

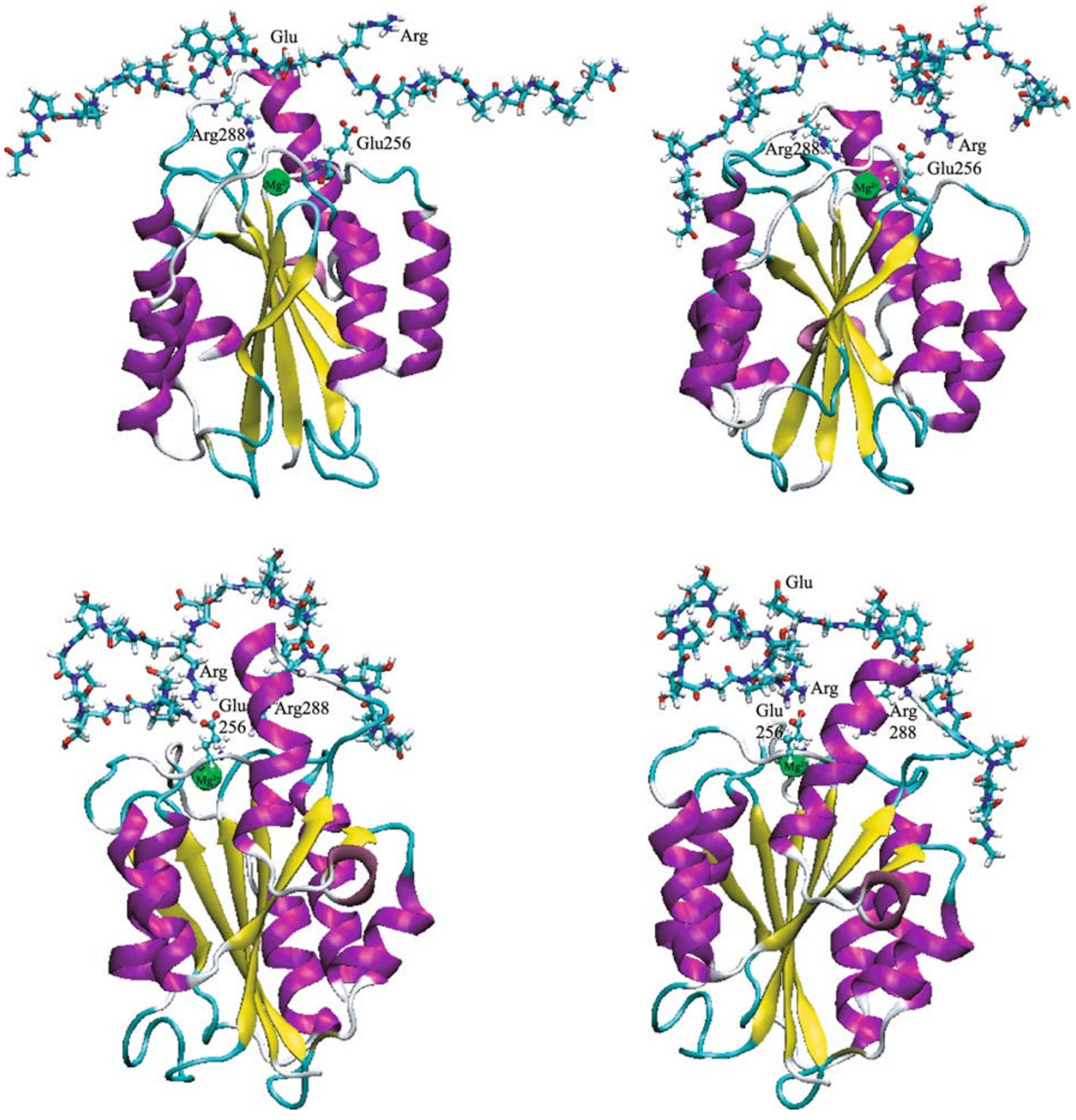

Figure 10. Single stranded collagen fragment (D-chain) in the binding pocket of α2A (1DZI.pdb). Snapshots are taken at four different states of the NAMD simulation.

induced activation model (Siljander et al., 2004). Our kinetic analysis reveals a congruence of calculated SPR curves fitted to raw SPR data using the two-state model, indicating a conformational shift during the binding event, as already predicted (Emsley et al., 2004). The affinities of metal-ion loaded α2A domains found here were in excellent agreement with previous data published by Calderwood et al. (Calderwood et al., 1995), who described approximate kinetic constants (k_{on} = 6.7 × 10^4 M^{-1} s^{-1}, k_{off} = 1.2 × 10^{-3} M^{-1} s^{-1} and K_D = 0.18 μM) using a simple association model for the α2A integrin domain interaction with collagen type I in the presence of 1 mM Mn^{2+}. The association rates calculated from our SPR data show that Co^{2+} ions have the strongest impact on the interaction, exhibited by a higher k_{on} value in comparison to other cations. This result demonstrates that the association is faster in the presence of Co^{2+} ions, but the high k_{off} value reveals fast dissociation of the complex under these conditions as well. In contrast, Mn^{2+} ions seem to stabilize the open, high-affinity form much better, as reported by the low dissociation constant. However, in contrast to Co^{2+} the

association rate in the presence of Mn^{2+} ions is small, implying that the complex formation is slower than in the presence of other cations. Compared to Mn^{2+} and Co^{2+} a weaker complex was formed in the presence of Mg^{2+}, as shown by the high dissociation rate (Table 1). This result is in full agreement with the data published by Humphries, 2002 (Humphries, 2002), reporting that Mn^{2+} promotes higher levels of ligand binding than Mg^{2+}. Obviously kinetic parameters of the collagen-α2A complex formation are determined by the nature of the available cations. Therefore, regulation of the cation concentration appears to provide a powerful mechanism for fine-tuning of the collagen-α2A interaction. In combination with recently discovered products (Valdramidou et al., 2008), showing the great impact of competition of different divalent cations on the common action of integrin α2 and β1 domains, our data provide further insights into the processes regulating the collagen-integrin interaction. The self-association behaviour of smaller and larger collagen strands was analyzed with MD-simulations and AFM experiments. The data are in agreement with results obtained by other methods. The 21mer collagen fragment has a melting temperature of 2°C (Emsley et al., 2004). The introduction of additional GPO triplets at each end of the sequence promotes the formation of a stable triple-helical structure (Morton et al., 1997; Knight et al., 1998). The loss of stability based on the replacement of GPO 3mer peptides by other sequences (Persikov et al., 2005). The stabilizing effect of peptide elongation is described in the literature. Therefore, the triple-helical structure formation of the 42mer collagen-peptide is much more likely than that of the 21mer. According to our MD-simulations a corresponding 33mer collagen-peptide also shows a significant tendency to form triple helices but this tendency is much lower than in the case of the 42mer peptide.

GPC triplets were introduced at the N and C terminus of the 42mer collagen fragment to allow cross-linking for polymer formation which is necessary for many biological activities (Knight et al., 1998). These structures are described to be most feasible for examinations, according to the architecture of integrin recognition sites for fibrillar collagen fragments (Siljander et al., 2004).

The investigation of smaller collagen fragments reveals that α2A interacts only with structures of higher molecular weight. No significant binding was detected in our SPR experiments with the 21mer collagen fragment. The SPR results obtained for the 42mer collagen fragment and α2A which are comparable to the results when collagen type I is interacting with this integrin domain underlines the higher physiological relevance of larger collagen fragments. Previous studies have also described that no binding occurs between α2A and collagen fragments after heat treatment which destroys the triple-helical structures (Knight et al., 1998).

AFM is one of the most suitable methods to examine fibrillar collagen strands (Elliott et al., 2005, 2007; Plant et al., 2009). Our AFM measurements demonstrate that the examined collagen fragments (21mer and 42mer) differ significantly in their shape and size (Fig. 2A and 2B). Due to the low heat stability of short triple-helical molecules, the smaller fragment did not aggregate into higher ordered structures (Knight et al., 1998).

Valuable hints concerning weak binding between the 21mer collagen fragment and α2A could be detected by NMR (Fig. 3A and 3B). It was possible to further analyse these hints by MD simulations. It is remarkable that the same single stranded collagen fragment shows a different binding behaviour in our MD simulations depending on the fragment's position in the collagen binding pocket of α2A. The difference in the binding performance of B- and D-chains is of special interest. In both cases, the arginine residue of the single-stranded collagen plays a crucial role, but only the D-chain forms a solid complex in our MD simulations. Comparison of the snapshots in Fig. 9 and Fig. 10 provides an answer for this difference. Besides the important Arg-Glu interaction, a number of additional intermolecular contacts like hydrogen bonds must exists. As can be clearly seen in Fig. 9, a major part of the B-chain is not able to establish such contacts during the whole MD simulation. The MD trajectory of the D-chain matches perfectly with our NMR observations of binding between the single-stranded collagen and α2A. The weak interactions between D-chain and α2A highlight special aspects of the intermolecular rendezvous between collagen and integrin.

The relevant support of the cation and intrinsic stability of the triple-helical strand does not play a role in this border-line binding process with a single-stranded collagen fragment. Particularly with regard to the initial contact between α2A and collagen fragments our results show that the arginine-residue (Arg12 of the 21mer collagen fragment) is of great importance. Only this collagen fragment residue and some hydrogen bonds mediate the interaction between the 21mer collagen fragment and α2A. Therefore, specific binding is indeed weakened significantly. Although single-stranded collagen fragments have to be considered as weak binding ligands, our findings provide detailed information on the interaction modes of artificial collagen fragments at a sub-molecular level. On the basis of these results we will analyse the biological impact of biological acitive collagen fragments in a strategic combination of NMR and molecular modeling methods as successfully carried out in other ligand-receptor interaction studies (Melacini et al., 2000; Siebert et al., 2002, 2003, 2005; Wu et al., 2007; Siebert et al., 2009; Bhunia et al., 2010). Furthermore, additional SPR experiments, quantum chemical calculations (Siebert et al., 2001; van Lenthe et al., 2004) (Supplemental Fig. 5) and an AFM-guided monitoring of the collagen fragment dependent chondrocyte differentiation will provide more valuable insights (Supplemental Fig. 6) about the structure-function relationship of collagen frag-

ments and their potential use as therapeutics (Oesser et al., 1999; Moskowitz, 2000; Humphries, 2002; Hynes, 2002; Oesser and Seifert, 2003; Bello and Oesser, 2006; Sweeney et al., 2008).

Since the interaction of α2β1 integrin with collagen is a part of the extracellular matrix signal transduction cascade it regulates many different cell functions, e.g., the platelet-collagen interaction during hemostasis (Grzesiak and Pierschbacher, 1995; Herr and Farndale, 2009), tumor cell proliferation and migration (Grzesiak and Bouvet, 2008), as well as contacts between chondrocytes and the extracellular matrix (Loeser, 2000) in particular cartilage. Therefore, a detailed understanding of the fine-tuning of collagen binding by tight regulation of α2A might be a potential tool for therapeutic purposes with beneficial effects on wound healing, development of new anti-tumor agents and prevention of degenerative diseases like osteoarthrosis (Bello and Oesser, 2006).

MATERIALS AND METHODS

The 42mer peptide

The 42mer peptide (GPCGPOGPOGPOGPOGPOGFOGERGPOG-POGPOGPOGPOGPC) and the 21mer peptide (GPOGPOGFO-GERGPOGPOGPO) were chemically synthesized on a solid-phase peptide synthesizer, and purified to homogeneity on an HPLC column.

The synthesized collagen fragments were purchased from the following suppliers: German Cancer Research Center (DKFZ), Germany (21mer) and Activotec, UK (42mer). The α2A domain was produced in the lab of M. Humphries.

SPR-experiments with 42mer and 21mer collagen fragments

The binding kinetics of α2A to immobilized collagen fragments were measured with a XPR36 ProteOn system (BioRad, Germany). Fragments were immobilized on a GLM Sensor chip (BioRad) according to the supplier's protocol using an amine coupling kit (BioRad). All steps were carried out at 25°C with a flow rate of 30 µL/min and 5 min contact time. Briefly, different channels of the chip were activated with EDC-sNHS solution. Collagen fragments in 10 mM acetate buffer pH = 4.5 were immobilized on chosen channels followed by deactivation with ethanolamine. Phosphate-buffered saline pH 7.4 containing 0.005% Tween 20 (PBS-T) was used as running buffer. Immobilization levels up to 1900 response units (RU) were obtained. For interaction measurements Tris base buffered saline pH 7.4 containing 0.005% Tween 20 (TBS-T) was used as running buffer instead of PBS-T, in order to prevent chelating of the divalent cations. Kinetic response data were collected for α2A at five concentrations (10, 20, 50, 100 and 200 nM in TBS-T), which were injected simultaneously in parallel channels with 2 mM $MgCl_2$ at a flow rate of 100 µL/min for 1min association phase followed by 5 min dissociation phase at 25°C. The effect of divalent cations on the interaction was further studied using 100 nM of α2A and 2 mM of $CoCl_2$, $MnCl_2$, and $MgCl_2$, respectively. For control studies α2A was immobilized under similar conditions.

All data were analyzed by the interspot reference function of the XPR36 software (BioRad). The software allows the calculation of kinetic constants (association rate (k_{on}), dissociation rate (k_{off}), and the K_D value) by simultaneously fitting the sensograms obtained at different concentrations of the analyte to a single value for each set of curves. The kinetic analysis was carried out using a two-state model for interaction in which the conformation changes upon ligand-analyte binding.

AFM-analysis of 21mer and 42mer collagen fragments

AFM was performed in tapping mode using an MFP-3D-Bio atomic force microscope (Atomic force, Germany). Collagen fragments were dissolved in pure water at a concentration of 10 ng/mL. The fragment solution was absorbed onto mica discs (Plano, Germany), which were glued on glass slides. After 15 min incubation at room temperature, the loaded mica surfaces were dried with nitrogen. All samples were imaged under air in tapping mode with OMCL-AC240TS-W2 (Atomic force) cantilevers. The data were processed using MFP-3D interface built on IGOR PRO version 6.02A.

Solid phase assays with collagen fragments

Solid phase assays were carried out as described in the literature (Calderwood et al., 1995) with minor modifications. Briefly 96-well microtiter plates (Nunc) were coated with 10 µg/mL collagen type I (PureCol, Nutricon) or 42mer collagen fragment (Activotec) in TBS buffer containing 2 mM $MgCl_2$ at 4°C overnight followed by a blocking step with TBS buffer containing 5% BSA and 2 mM MgCl for 1 h at 37°C. After washing with a buffer (TBS, 1% BSA, 2 mM $MgCl_2$) GST-α2A integrin (100 µg/mL in TBS) was added. GST was used as control. The plates were incubated for 1 h at room temperature. Then after washing an anti-GST antibody solution (Novagen, 1:8000 in washing buffer) was added and incubated for 1 h at room temperature followed by three washing steps and subsequent addition of a biotinylated anti-mouse antibody (Dianova, 1:5000 in washing buffer). The plates were incubated for 1 h at room temperature. After washing and 30 min incubation with streptavidin-coated alkaline phosphatase (Dianova, 1:500 in washing buffer) nitrophenyl phosphate solution (1 mg/mL) was added and the reaction was stopped after 30 min with 3 M NaOH. The plates were measured at 405 nm using an ELISA reader (Labsystems).

AFM-analysis of chondrocytes

Primary equine chondrocytes were cultivated in culture dishes as described elsewhere. Subconfluent cells were fixed with ice-cold methanol and dried under nitrogen. Measurements were performed in tapping mode as described for analysis of collagen fragments.

NMR spectroscopy

D-experiments: Binding of the collagen fragments to α2A was studied by monitoring changes in 1D ^1H NMR spectra, and by measuring saturation transfer difference (STD) spectra. These titration experiments with various collagen fragments were carried out at 700 and 900 MHz field strength for different α2A samples and various ($\leqslant$ 10) concentrations of the collagen fragments. The α2A

concentration was fixed at 3 mM in all NMR experiments. For reference, a first α2A sample in PBS buffer was used to record the ^{1}H-NMR chemical shifts of the collagen-free protein sample. The 1D-NMR spectrum for the sample with the highest ligand/protein ratio (= end point of titration) was recorded by dissolving the collagen fragments (at a concentration of 30 mM) in 0.5 mL of α2A containing solution.

D-Experiments: Samples were prepared by dissolving lyophilized α2A in 0.5 mL 20 mM phosphate buffer (90% H_2O, 10% D_2O). ^{1}H-NMR spectra were recorded on Bruker AVANCE II 700 and 900 MHz spectrometers. 2D-TOCSY and 2D-NOESY spectra were recorded with 256(F1) × 1024(F2) complex data points and a spectral width of 9000 Hz. 64 scans were used per increment with an inter-scan recovery delay of 1 s. We used zero-filling to 1024(F1) × 2048(F2) data points prior to Fourier transformation, and baseline correction in both dimensions. The corresponding shift was optimized for the different spectra. 2D-TOCSY spectra were acquired using MLEV-17 mixing for 60 ms. The 2D-NOESY experiments were performed with mixing times of 50, 125 and 200 ms (Diercks et al., 2001; Siebert et al., 2002, 2003, 2005).

Molecular dynamics simulations

Molecular dynamics (MD) simulations were performed using NAMD2 2.6 and the CHARMM22 force field parameters (MacKerell et al., 1998). Starting coordinates were obtained from the 2.1-Å resolution X-ray crystal structure of the complex between the integrin α2A domain and a triple-helical part of collagen, PDB entry: 1DZI (Emsley et al., 2000; Humphries, 2002). The structure includes three strands of collagen, which are here referred to as chain B, C, and D, respectively. A Co^{2+} ion is reported in the crystal structure at the interface between the collagen and the α2A integrin domain (called chain A), specifically coordinated by Glu11 of one of the collagen strands. In all MD simulations Mg^{2+} was substituted for Co^{2+}. The systems were all solvated in a sufficiently large water box (approximately $70 \times 70 \times 65$ Å^3) using the SOLVATE plugin of VMD (Humphrey et al., 1996). NaCl was added to the simulation box in all systems at 100 mM concentration. The number of ions was adjusted to achieve electro-neutrality. The total atom count of the systems is about 30,000 atoms. The CHARMM22 set of force-field parameters (MacKerell et al., 1998; Brooks et al., 2009) and the TIP3 model of water (Jorgensen et al., 1986) were used in all the simulations. The parameters for hydroxyproline were developed starting from proline and adopting the hydroxy parameters from similar chemical groups in the force field. Short simulations of an isolated hydroxyproline in water were carried out to ensure that the parameters reproduce a natural structural behaviour of this modified residue.

Four independent simulations were performed in order to investigate the stability and mode of interaction between collagen and integrin. The first simulation included the collagen fragment in its complete triple-helical form as present in the crystal structure. The other three simulations comprised α2A and only one of the different collagen strands.

After an initial short minimization and water relaxation simulations, during which the protein components of the system were constrained to their initial PDB conformation, the system was simulated for 10 ns as an NPT ensemble (constant pressure and temperature), and the structures were saved every 1 ps. The target pressure was set to 1.0 atm, the temperature to 310 K, and the time-step to 1 fs. Constant pressure was maintained by the Langevin piston Nose-Hoover method (Feller et al., 1995). A Langevin damping coefficient, gamma, of 1.0 ps^{-1} was used for temperature control. The particle mesh ewald (PME) method (Darden et al., 1999) was employed to calculate electrostatic forces without truncation.

An additional set of MD simulations for triple-helical collagen fragments (20–30 residues), as well as for the complex of the collagen fragment and α2A (also based on the X-ray structure 1DZI.pdb) were performed with GROMACS 3.1.4 (van der Spoel et al., 2005) in an explicit box of water, in order to test the effect of different force fields. The applied force field for these simulations was GROMOS 96 ffG43a1, along with the SPC model for water. Several MD simulations (up to 10 ns) of 3 collagen trimeric units (chain length up to 30 residues, twist: 21 residues, length: 59 Å) were performed at T = 300 K using the PME method.

Comparison of force field parameters

Additional comparative force field calculations especially for the ion-parameterization were carried out with the MM + and CHARMM27 force fields, which are included in the Hyperchem 8.0 professional software package.

ABBREVIATIONS

AFM, atom force microscopy; MD, molecular dynamics; PME, particle mesh ewald; RU, response units; STD, saturation transfer difference; SPR, surface plasmon resonance

REFERENCES

Bello, A.E., and Oesser, S. (2006). Collagen hydrolysate for the treatment of osteoarthritis and other joint disorders: a review of the literature. Curr Med Res Opin 22, 2221–2232.

Berisio, R., Vitagliano, L., Mazzarella, L., and Zagari, A. (2002). Crystal structure of the collagen triple helix model [(Pro-Pro-Gly)(10)](3). Protein Sci 11, 262–270.

Bhunia, A., Vivekanandan, S., Eckert, T., Burg-Roderfeld, M., Wechselberger, R., Romanuka, J., Bachle, D., Kornilov, A.V., von der Lieth, C.W., Jimenez-Barbero, J., *et al.* (2010). Why structurally different cyclic peptides can be glycomimetics of the HNK-1 carbohydrate antigen. J Am Chem Soc 132, 96–105.

Brooks, B.R., Brooks, C.L., Mackerell, A.D., Nilsson, L., Petrella, R.J., Roux, B., Won, Y., Archontis, G., Bartels, C., Boresch, S., *et al.* (2009). CHARMM: The biomolecular simulation program. J Comput Chem 30, 1545–1614.

Calderwood, D.A., Tuckwell, D.S., and Humphries, M.J. (1995). Specificity of integrin I-domain-ligand binding. Biochem Soc Trans 23, 504S.

Coe, A.P., Askari, J.A., Kline, A.D., Robinson, M.K., Kirby, H., Stephens, P.E., and Humphries, M.J. (2001). Generation of a minimal alpha5beta1 integrin-Fc fragment. J Biol Chem 276, 35854–35866.

Darden, T., Perera, L., Li, L., and Pedersen, L. (1999). New tricks for modelers from the crystallography toolkit: the particle mesh Ewald algorithm and its use in nucleic acid simulations. Structure 7, R55–60.

Dickeson, S.K., Walsh, J.J., and Santoro, S.A. (1997). Contributions

of the I and EF hand domains to the divalent cation-dependent collagen binding activity of the alpha2beta1 integrin. J Biol Chem 272, 7661–7668.

Diercks, T., Coles, M., and Kessler, H. (2001). Applications of NMR in drug discovery. Curr Opin Chem Biol 5, 285–291.

Elliott, J.T., Woodward, J.T., Langenbach, K.J., Tona, A., Jones, P.L., and Plant, A.L. (2005). Vascular smooth muscle cell response on thin films of collagen. Matrix Biol 24, 489–502.

Elliott, J.T., Woodward, J.T., Umarji, A., Mei, Y., and Tona, A. (2007). The effect of surface chemistry on the formation of thin films of native fibrillar collagen. Biomaterials 28, 576–585.

Emsley, J., Knight, C.G., Farndale, R.W., and Barnes, M.J. (2004). Structure of the integrin alpha2beta1-binding collagen peptide. J Mol Biol 335, 1019–1028.

Emsley, J., Knight, C.G., Farndale, R.W., Barnes, M.J., and Liddington, R.C. (2000). Structural basis of collagen recognition by integrin alpha2beta1. Cell 101, 47–56.

Feller, S.E., Zhang, Y.H., Pastor, R.W., and Brooks, B.R. (1995). Constant-pressure molecular-dynamics simulation—the Langevin Piston Method. J Chem Phys 103, 4613–4621.

Grzesiak, J.J., and Bouvet, M. (2008). Activation of the alpha2beta1 integrin-mediated malignant phenotype on type I collagen in pancreatic cancer cells by shifts in the concentrations of extracellular Mg^{2+} and Ca^{2+}. Int J Cancer 122, 2199–2209.

Grzesiak, J.J., and Pierschbacher, M.D. (1995). Shifts in the concentrations of magnesium and calcium in early porcine and rat wound fluids activate the cell migratory response. J Clin Invest 95, 227–233.

Herr, A.B., and Farndale, R.W. (2009). Structural insights into the interactions between platelet receptors and fibrillar collagen. J Biol Chem 284, 19781–19785.

Huizinga, E.G., Martijn van der Plas, R., Kroon, J., Sixma, J.J., and Gros, P. (1997). Crystal structure of the A3 domain of human von Willebrand factor: implications for collagen binding. Structure 5, 1147–1156.

Humphrey, W., Dalke, A., and Schulten, K. (1996). VMD: visual molecular dynamics. J Mol Graph 14, 33–38, 27–38.

Humphries, J.D., Askari, J.A., Zhang, X.P., Takada, Y., Humphries, M. J., and Mould, A.P. (2000). Molecular basis of ligand recognition by integrin alpha5beta 1. II. Specificity of arg-gly-Asp binding is determined by Trp157 OF THE alpha subunit. J Biol Chem 275, 20337–20345.

Humphries, M.J. (2002). Insights into integrin-ligand binding and activation from the first crystal structure. Arthritis Res 4 Suppl 3, S69–78.

Hynes, R.O. (2002). Integrins: bidirectional, allosteric signaling machines. Cell 110, 673–687.

Ichikawa, O., Osawa, M., Nishida, N., Goshima, N., Nomura, N., and Shimada, I. (2007). Structural basis of the collagen-binding mode of discoidin domain receptor 2. EMBO J 26, 4168–4176.

Jorgensen, W.L., Chandrasekhar, J., Buckner, J.K., and Madura, J.D. (1986). Computer simulations of organic reactions in solution. Ann N Y Acad Sci 482, 198–209.

Kiedzierska, A., Smietana, K., Czepczynska, H., and Otlewski, J. (2007). Structural similarities and functional diversity of eukaryotic discoidin-like domains. Biochim Biophys Acta 1774, 1069–1078.

Kim, J.K., Xu, Y., Xu, X., Keene, D.R., Gurusiddappa, S., Liang, X., Wary, K.K., and Hook, M. (2005). A novel binding site in collagen type III for integrins alpha1beta1 and alpha2beta1. J Biol Chem 280, 32512–32520.

Knight, C.G., Morton, L.F., Onley, D.J., Peachey, A.R., Messent, A.J., Smethurst, P.A., Tuckwell, D.S., Farndale, R.W., and Barnes, M.J. (1998). Identification in collagen type I of an integrin alpha2 beta1-binding site containing an essential GER sequence. J Biol Chem 273, 33287–33294.

Leitinger, B., and Hohenester, E. (2007). Mammalian collagen receptors. Matrix Biol 26, 146–155.

Loeser, R.F. (2000). Chondrocyte integrin expression and function. Biorheology 37, 109–116.

MacKerell, A.D., Bashford, D., Bellott, M., Dunbrack, R.L., Evanseck, J.D., Field, M.J., Fischer, S., Gao, J., Guo, H., Ha, S., *et al*. (1998). All-atom empirical potential for molecular modeling and dynamics studies of proteins. J Phys Chem B 102, 3586–3616.

Melacini, G., Bonvin, A.M.J.J., Goodman, M., Boelens, R., and Kaptein, R. (2000). Hydration dynamics of the collagen triple helix by NMR. J Mol Biol 300, 1041–1048.

Morton, L.F., Peachey, A.R., Knight, C.G., Farndale, R.W., and Barnes, M.J. (1997). The platelet reactivity of synthetic peptides based on the collagen III fragment alpha1(III)CB4. Evidence for an integrin alpha2beta1 recognition site involving residues 522–528 of the alpha1(III) collagen chain. J Biol Chem 272, 11044–11048.

Moskowitz, R.W. (2000). Role of collagen hydrolysate in bone and joint disease. Semin Arthritis Rheum 30, 87–99.

Nahshol, O., Bronner, V., Notcovich, A., Rubrecht, L., Laune, D., and Bravman, T. (2008). Parallel kinetic analysis and affinity determination of hundreds of monoclonal antibodies using the ProteOn XPR36. Anal Biochem 383, 52–60.

Nishida, N., Sumikawa, H., Sakakura, M., Shimba, N., Takahashi, H., Terasawa, H., Suzuki, E., and Shimada, I. (2003). Collagen-binding mode of vWF-A3 domain determined by a transferred cross-saturation experiment. Nat Struct Biol 10, 53–58.

Oesser, S., Adam, M., Babel, W., and Seifert, J. (1999). Oral administration of (14)C labeled gelatin hydrolysate leads to an accumulation of radioactivity in cartilage of mice (C57/BL). J Nutr 129, 1891–1895.

Oesser, S., and Seifert, J. (2003). Stimulation of type II collagen biosynthesis and secretion in bovine chondrocytes cultured with degraded collagen. Cell Tissue Res 311, 393–399.

Persikov, A.V., Ramshaw, J.A., and Brodsky, B. (2005). Prediction of collagen stability from amino acid sequence. J Biol Chem 280, 19343–19349.

Plant, A.L., Bhadriraju, K., Spurlin, T.A., and Elliott, J.T. (2009). Cell response to matrix mechanics: focus on collagen. Biochim Biophys Acta 1793, 893–902.

Romijn, R.A., Bouma, B., Wuyster, W., Gros, P., Kroon, J., Sixma, J.J., and Huizinga, E.G. (2001). Identification of the collagen-binding site of the von Willebrand factor A3-domain. J Biol Chem 276, 9985–9991.

Siebert, H.C., Adar, R., Arango, R., Burchert, M., Kaltner, H., Kayser, G., Tajkhorshid, E., VonderLieth, C.W., Kaptein, R., Sharon, N., *et al*. (1997). Involvement of laser photo-CIDNP(chemically induced dynamic nuclear polarization)-reactive amino acid side chains in ligand binding by galactoside-specific lectins in solution. Eur J Biochem 249, 27–38.

Siebert, H.C., Andre, S., Lu, S.Y., Frank, M., Kaltner, H., van Kuik, J. A., Korchagina, E.Y., Bovin, N., Tajkhorshid, E., Kaptein, R., *et al*.

(2003). Unique conformer selection of human growth-regulatory lectin galectin-1 for ganglioside GM1 versus bacterial toxins. Biochemistry 42, 14762–14773.

Siebert, H.C., Born, K., Andre, S., Frank, M., Kaltner, H., von der Lieth, C.W., Heck, A.J., Jimenez-Barbero, J., Kopitz, J., and Gabius, H.J. (2005). Carbohydrate chain of ganglioside GM1 as a ligand: identification of the binding strategies of three 15 mer peptides and their divergence from the binding modes of growth-regulatory galectin-1 and cholera toxin. Chemistry 12, 388–402.

Siebert, H.C., Lu, S.Y., Frank, M., Kramer, J., Wechselberger, R., Joosten, J., Andre, S., Rittenhouse-Olson, K., Roy, R., von der Lieth, C.W., *et al*. (2002). Analysis of protein-carbohydrate interaction at the lower size limit of the protein part (15-mer peptide) by NMR spectroscopy, electrospray ionization mass spectrometry, and molecular modeling. Biochemistry 41, 9707–9717.

Siebert, H.C., Lu, S.Y., Wechselberger, R., Born, K., Eckert, T., Liang, S., von der Lieth, C.W., Jimenez-Barbero, J., Schauer, R., Vliegenthart, J.F., *et al*. (2009). A lectin from the Chinese bird-hunting spider binds sialic acids. Carbohydr Res 344, 1515–1525.

Siebert, H.C., Tajkhorshid, E., and Dabrowski, J. (2001). Barrier to rotation around the C-sp(2)-C-sp(2) bond of the ketoaldehyde enol ether MeC(O)CH = CH-OEt as determined by C-13 NMR and ab initio calculations. J Phys Chem A 105, 8488–8494.

Siljander, P.R., Hamaia, S., Peachey, A.R., Slatter, D.A., Smethurst, P.A., Ouwehand, W.H., Knight, C.G., and Farndale, R.W. (2004). Integrin activation state determines selectivity for novel recognition sites in fibrillar collagens. J Biol Chem 279, 47763–47772.

Sweeney, S.M., Orgel, J.P., Fertala, A., McAuliffe, J.D., Turner, K.R., Di Lullo, G.A., Chen, S., Antipova, O., Perumal, S., Ala-Kokko, L., *et al*. (2008). Candidate cell and matrix interaction domains on the collagen fibril, the predominant protein of vertebrates. J Biol Chem 283, 21187–21197.

Valdramidou, D., Humphries, M.J., and Mould, A.P. (2008). Distinct roles of beta1 metal ion-dependent adhesion site (MIDAS), adjacent to MIDAS (ADMIDAS), and ligand-associated metal-binding site (LIMBS) cation-binding sites in ligand recognition by integrin alpha2beta1. J Biol Chem 283, 32704–32714.

van der Spoel, D., Lindahl, E., Hess, B., Groenhof, G., Mark, A.E., and Berendsen, H.J. (2005). GROMACS: fast, flexible, and free. J Comput Chem 26, 1701–1718.

van Lenthe, J.H., den Boer, D.H.W., Havenith, R.W.A., Schauer, R., and Siebert, H.C. (2004). Ab initio calculations on various sialic acids provide valuable information about sialic acid-specific enzymes. J Mol Struct (Theochem) 677, 29–37.

Vogel, W.F., Abdulhussein, R., and Ford, C.E. (2006). Sensing extracellular matrix: an update on discoidin domain receptor function. Cell Signal 18, 1108–1116.

Wu, A.M., Singh, T., Liu, J.H., Krzeminski, M., Russwurm, R., Siebert, H.C., Bonvin, A.M., Andre, S., and Gabius, H.J. (2007). Activity-structure correlations in divergent lectin evolution: fine specificity of chicken galectin CG-14 and computational analysis of flexible ligand docking for CG-14 and the closely related CG-16. Glycobiology 17, 165–184.

Xiong, J.P., Stehle, T., Zhang, R., Joachimiak, A., Frech, M., Goodman, S.L., and Arnaout, M.A. (2002). Crystal structure of the extracellular segment of integrin alpha Vbeta3 in complex with an Arg-Gly-Asp ligand. Science 296, 151–155.

